NASA Technical Memorandum 86940

Ribbon-Burner Simulation of the T-700 Turbine Shroud Section for Ceramic-Lined Seals Research

J.K. Little
Arnold Air Force Station
Tullahoma, Tennessee

G.P. Allen, G. McDonald, and R.C. Hendricks
Lewis Research Center
Cleveland, Ohio

Prepared for the
Ninth Annual Conference on Composites and
Advanced Ceramic Materials
sponsored by the American Ceramic Society
Cocoa Beach, Florida, January 20–24, 1985

NASA

RIBBON-BURNER SIMULATION OF T-700 TURBINE SHROUD FOR CERAMIC-LINED SEALS RESEARCH

J.K. Little
Arnold Air Force Station
Tullahoma, Tennessee 37389

and

G.P. Allen, G. McDonald, and R.C. Hendricks
National Aeronautics and Space Administration
Lewis Research Center
Cleveland, Ohio 44135

SUMMARY

Presented herein are the results of experimental and analytical tests to determine the acceptability of a ribbon burner to simulate the environment of the turbine shroud seal section of the T-700 turboshaft engine. The calculated values reveal that the ribbon burner establishes at least as harsh a thermal environment as is present at any time within the first-stage, high-pressure turbine shroud. Since ceramic-coated test pieces of proposed T-700 ceramic-lined shrouds have endured upward of 2000 cycles within the ribbon-burner test rig, the shrouds should be able to endure the thermal demands of the T-700 turbine.

INTRODUCTION

A theory has been proposed that lining turbine tip shrouds with ceramic insulating materials will allow increased performance levels within the T-700 engine. The theory seems sound, but problems have been encountered in establishing a coating that will withstand the harsh thermal environment of the turbine. Although ceramics are well known for their ability to withstand high temperatures, they also lack ductility and this is where the problem occurs. If a ceramic-lined shroud is subjected to a large thermal gradient, the hot (cold) ceramic outer surface will tend to expand (contract) before the shroud material does. Also, once steady-state conditions have been achieved, the shroud material will expand more than the ceramic because of the variance in thermal expansion coefficients. These conditions create stresses within the relatively brittle ceramic that cause it to crack and separate from the shroud. Therefore in creating a shroud design the important areas of concern are its ability to withstand the surface heat fluxes found in transient performance and the variance in steady-state conditions.

A design, constrained to existing hardware, has been developed and tested that seems to fulfill the thermal requirements of the T-700 turboshaft engine (fig. 1). The modification to shroud components consisted of adding a 1-mm (0.04-in) layer of ZrO_2-$8Y_2O_3$ connected to the nominally 0.89-mm (0.035-in) thick Haynes 25 substrate by a 1-mm (0.04-in) layer of NiCoCrAlX bonding material (ref. 1). The thicknesses of the layers are important. The thinner the ceramic, the lower the thermal stresses will be. A thick ceramic tends to

insulate more and cause larger thermal gradients (and therefore higher stresses) than thinner layers. If the ceramic is made too thin, however, the purpose of putting the ceramic on the shrouds (thermal insulation) can easily be defeated. This compromising situation, along with the requirement to fit existing engine components, limited the design. This investigation proved that it was possible to arrive at a design compromise and proved the survivability of the design compromise in engine tests (ref. 1).

SYMBOLS

A	cross-sectional area
C_1	constant
g_c	gravitational constant
h_c	convection coefficient
k_f	thermal conductivity of film region
k_2	thermal conductivity of ceramic region
k_3	thermal conductivity of bond-coat region
k_4	thermal conductivity of substrate or stainless steel region
L	length over which convective flow acts
M	Mach number
Pr_f	Prandtl number of film region
$P_{s,4.0}$	static pressure at station 4
$P_{T,4.0}$	total pressure at station 4
q	heat transfer rate
q''	heat flux, q/A
q''_{ss}	steady-state heat flux
q''_{trans}	transient heat flux
R	universal gas constant
Re_f	Reynolds number of film region
R_f	thermal resistance of film region
R_2	thermal resistance of ceramic region
R_3	thermal resistance of bond-coat region

R_4	thermal resistance of substrate or stainless steel region
T_a	temperature of gas stream
T_b	temperature of ceramic surface in engine tests
T_c	temperature of ceramic - bond-coat interface
T_d	temperature of bond-coat - shroud interface
T_e	temperature of back side of shroud
$T_{s,4.0}$	static temperature at station 4.0
$T_{s,4.1}$	static temperature at station 4.1
$T_{T,4.1}$	total temperature at station 4.1
$T_{T,3.0}$	total temperature at station 3.0
T_f	temperature of film region
T_{flame}	temperature of ribbon-burner flame
T_{high}	temperature of gas stream or flame causing transients
$T_{interior}$	temperature of point inside of stainless steel region in ribbon-burner test
T_{low}	temperature of ceramic surface just prior to transient effect of T_{high}
$T_{surface}$	temperature of ceramic surface in ribbon-burner tests
t_2	thickness of ceramic region
t_3	thickness of bond-coat region
t_4	thickness of substrate or stainless steel region
u	velocity of flow causing convection
v	velocity
$W_{4.1}$	airflow at station 4.1
γ	ratio of specific heats
μ_f	dynamic viscosity of film region
ρ_a	density of gas stream
ρ_f	density of film region

Subscript:

ipp intermediate power point

TEST SPECIMEN AND APPARATUS

The ceramic-coated shroud modification (ref. 1) was simulated with specimens fabricated by plasma spraying 1-mm (0.04-in) ZrO_2-$8Y_2O_3$ over a 1-mm (0.04-in) NiCrAlY bond coat that had been plasma sprayed onto a 9.7 x 25.4 x 51 mm (0.38 x 1.0 x 2.0 in) stainless steel substrate. Thermocouple wires were led through the substrate, and a junction was formed at the bond-coat - substrate interface.

These specimens were tested in a ribbon-burner apparatus (ref. 2). In this rig (fig. 2) the test articles were automatically cycled in and out of the direct heat of the ribbon-burner flame and directly cooled with an ambient air jet. Ambient air, directed at the back side of the substrate, was used to control heating rates and overall temperature. Each heating cycle was held long enough to bring the test article to steady-state heating conditions, and each cooling cycle was held long enough to bring the test article to relatively uniform temperatures (3 and 2 min, respectively). All of the test artciles were cycled over 2000 times. If the burner created as harsh an environment as the T-700 engine, 2000 cycles would be more than adequate for the proposed engine tests.

THERMAL DATA

Because of the dearth of information on the thermal conditions within the T-700 turbine shroud seal section and despite the complexity of the problem,* simplistic computational procedures were used in comparing the ribbon burner and the shroud section. In both, quasi-steady, one-dimensional heat transfer through a flat plate was assumed to apply.

T-700 Shroud Seal Section

The temperatures required for heat transfer analysis of the T-700 shroud seal section were acquired from engine test data. The turbine inlet total temperature at station 4.1 ($T_{T,4.1}$) and the compressor discharge total temperature at station 3.0 ($T_{T,3.0}$) were the two direct measurements used (fig. 1). By using a Mach number specification provided by the engine manufacturer, $T_{T,4.1}$ was adjusted to a static temperature and used as the gas temperature facing the ceramic area of the seal. Since the air used to cool the back side of the turbine shroud is bled from station 3.0, $T_{T,3.0} \approx T_{s,3.0}$ was used as the back-side surface temperature. This assumption may have set the back-side temperature too low. The cooling air will gain heat going around the combustor

---

*Shroud heat transfer is complicated by variations in blade clearance, flow across and along the blade, coolant dumping, rotation, and throughflow (appendix A).

section, and the surface will be hotter than the surrounding cooling air. However, this error is conservative since it causes a high calculation of the heat transfer rate and therefore makes the engine environment appear harsher than it is.

Ribbon-Burner Test

Temperatures were measured at three points: the flame, the front face of the test article, and the bond-coat - substrate interface. From these temperatures the convection coefficient between the flame and the ceramic surface was calculated. The interface temperature was measured with a thermocouple partially embedded in the substrate, the ceramic surface temperature was measured with a pyrometer, and the flame temperature was measured by using both of these methods.

ANALYSIS

The investigation into the adequacy of the ribbon-burner test was broken down into two categories: steady state and transient. First, the steady-state conditions of the heat transfer through the liners were investigated at idle and intermediate speeds in the T-700 engine. These conditions were then compared with the steady-state condition used in the ribbon-burner tests. Second, and more important, transient heat transfers leading to the two steady-state engine conditions (idle and intermediate) were compared with the transient effects found in the ribbon burner. Transient thermal conditions create high thermal stresses that are major contributors to ceramic failure.

Details of the calculations and the assumptions associated with them can be found in the appendixes.

T-700 Model

The quasi-steady, one-dimensional heat transfer model is illustrated in figure 3. The heat transfer is determined from the material properties, geometry, and temperatures by

$$q'' = \frac{q}{A} = \frac{T_{s,4.1} - T_{s,3.0}}{1/h_c + t_2/k_2 + t_3/k_3 + t_4/k_4} \tag{1}$$

For a flat plate in turbulent flow the film coefficient becomes

$$h_c = 0.036 \left(\frac{k_f}{L}\right) Re_f^{0.8} Pr_f^{1/3} \tag{2}$$

Because the flow area was not known, a constant combining the loss coefficients, gas properties, and flow area was determined

$$C_1 = \left(\frac{W}{\rho M \sqrt{T_s}}\right)_{4.1} \tag{3}$$

where

$$W_{4.1} = \left(C_f \rho M A \sqrt{\gamma R T_{s,4.1}}\right)_{ipp} \tag{4}$$

was approximated from engine manufacturer's specifications at the intermediate power point (ipp), where $M = 0.3$. With these values, idle and intermediate conditions of interest were approximated (table I).

The quasi-steady relation used to calculate the transient flux assumes constant properties and no thermal inertia, with h_c given by equation (2).

$$q''_{trans} = h_c(T_{high} - T_{low}) \tag{5}$$

The initial transient heat flux is determined by setting T_{low} to the surface condition prior to the transient and T_{high} to the high temperature of the flow causing the transient. The iterated solutions of interest are summarized in table II.

Ribbon-Burner Test

The computational model of the specimens used to simulate the T-700 engine components is illustrated in figure 4. The quasi-steady analysis was applied. As the flame and cooling air jets impinged on and flowed about the specimen, nonuniform heat flow caused the transfer rate to be lower than the calculated value. Since the calculations affected by this error were made at the steady-state condition, where the temperatures throughout the block were high, the effect of radial flow was assumed to be negligible.

The results of these computations are given in table III. As can be seen, the burner simulation presents a harsher thermal environment than was anticipated for the T-700 shroud.

CONCLUSIONS

Keeping in mind the conservative approach taken in the analysis, the results reveal that the ribbon burner creates a harsher environment for the ceramic seal design than does the engine. Both the steady-state and transient responses were lower in the engine than they were in the ribbon burner. Since each of the test articles withstood over 2000 cycles in the ribbon burner, the ceramic shroud design in the T-700 engine should easily withstand a similar magnitude of thermal cycling and, in fact, did.

APPENDIX A

T-700 ENGINE ANALYSIS

Shroud Seal Problem

The primary purpose of a seal is to minimize fluid leakage and the secondary purpose is to enhance system stability. The thermomechanical and fluid physics aspects of shroud seals are both quite complex. To consider one without the other can lead to fatigue damage with associated catastrophic failures of ceramic components or increased leakages and instabilities.

Typical clearances in jet engine turbomachines are 0.5 mm (20 mil) for the turbine and 0.4 mm (15 mil) for the compressor. With a blade thickness of 2.5 to 13 mm (100 to 500 mil) the flow passages ($5 < L/c < 30$) are short channels but are still long enough to effect flow reattachment. As such the flow coefficients are probably of the order of 0.75 to 0.90, depending on the nature of the blade tip treatment. Realistically the L/c varies between 20 and <1, because of blade geometry, and so the flow attachment patterns are quite complicated.

Several factors are unknown: the effects of secondary flows due to flow over the airfoil; the flow coefficient for a leading-edge geometry with one boundary in motion; the airfoil leading- and trailing-edge effects; and the local velocities (Mach number), heating rates, effects of mass injection, turbulence level, etc., for the flow. For the thermomechanical aspects it is necessary to determine the coupled bending and shear loads such that, if a rub does occur, the blade can withstand the impact loading without catastrophic failure. It is also necessary to know the global rotor position with respect to the "case" or housing. Also unknown are how the low-frequency dynamics are coupled to the rub and the coupling of high-frequency chatter established upon asperity contacts and subsequent rebounding of the contacting surfaces. The entrained fluid and the sheared materials serve as lubricants for the "rub"; enter the multiphase fluid physics problem. The heat dissipated, the energy lost to material removal, surface fracture, etc., must be determined. These results must then be entered into the blade thermofatigue history.

Realizing the limitations of the burner test rig and the inability to properly simulate the heat transfer characteristics, we propose a simple one-dimensional, quasi-steady model.

Steady-State Analysis

The steady-state T-700 engine analysis was based on the following assumptions:

(1) Heat transfer is quasi-one-dimensional, with uniform surface conditions and constant thermophysical properties.

(2) The shroud section is approximately a flat plate with no contact resistance at material interfaces.

(3) The combustion gas temperature surrounding the ceramic (a) is at $T_{4.1}$ (turbine inlet temperature), (b) can be simulated by air, (c) is a perfect gas, and (d) is unaffected by blade rotation or coolant dumping.

(4) The back-side surface temperature of the shroud is $T_{3.0}$ and is unaffected by coolant injection or leakage.

The shroud heat transfer model and governing equations for steady state become

$$q = \frac{T_a - T_e}{R_f + R_2 + R_3 + R_4} \tag{A1}$$

where

$$R_f = \frac{1}{h_c A}; \quad R_2 = \frac{t_2}{k_2 A}; \quad R_3 = \frac{t_3}{k_3 A}; \quad R_4 = \frac{t_4}{k_4 A} \tag{A2}$$

Therefore

$$q'' = \frac{q}{A} = \frac{T_a - T_e}{\frac{1}{h_c} + \frac{t_2}{k_2} + \frac{t_3}{k_3} + \frac{t_4}{k_4}} \tag{A3}$$

and for a flat plate in turbulent flow

$$h_c = 0.36 \left(\frac{k_f}{L}\right) Re_f^{4/5} Pr_f^{1/3} \tag{A4}$$

where

$$Re_f = \frac{uL\rho_f}{\mu_f} \tag{A5}$$

and $L = 0.0191$ m (0.0625 ft) is the width of the shroud over which the flow is assumed to pass. The steady-state test data for the T-700 engine are given in table IV.

Calculations

Velocity at station 4.1. The static properties are determined from conventional gas dynamics (ref. 4) and according to the engine manufacturer the Mach number at station 4.1 at intermediate power is 0.3. The flow area is an uncertainty, and the Mach number for idle is determined by assuming that all such unknowns are constant. Using one-dimensional flow gives

$$W_{4.1} = (\rho u A)_{4.1,ipp} = \left(C_f \rho M A \sqrt{\gamma g_c R T_s}\right)_{4.1,ipp} \tag{A6}$$

and combining knowns gives the constant

$$C_1 = \left(\frac{W}{\rho M \sqrt{T_s}} \right)_{4.1,ipp} \tag{A7}$$

The Mach number at idle can be iteratively calculated as

$$M = \left(\frac{W}{\rho C_1 \sqrt{T_s}} \right)_{4.1} \tag{A8}$$

and the local velocity becomes

$$u = \left(M \sqrt{\gamma g_c R T_s} \right)_{4.1} \tag{A9}$$

The calculations, which are based on the properties of air (ref. 6) ($R = 53.34$, $\gamma = 1.4$, $g_c = 32.174$), are summarized in table V.

Heat Transfer

The surface temperature T_b is estimated and used to calculate the heat transfer through the shroud from equations (A1) to (A5).

$$q'' = h_c(T_a - T_b) \tag{A10}$$

and a new value for T_b is then calculated,

$$T_b = T_a - \frac{q''}{h_c} \tag{A11}$$

The process is repeated until the calculations converge.

Intermediate power. An educated initial guess for T_b is 1200 K (2160 °R), and several iterations lead the calculation procedure to the final steps. For the properties of air (ref. 5) and the previously iterated value of T_b (1180 K; 2124 °R), the Prandtl number, the thermal conductivity, and the viscosity are evaluated at the film temperature.

$$T_f = 0.5(T_a + T_b) = 1294 \text{ K } (2329 \text{ °R}) \tag{A12}$$

$$Pr_f = 0.725 \tag{A13}$$

$$k_f = 0.08 \text{ W/K m } (0.046 \text{ Btu/hr ft °R}) \tag{A14}$$

$$\mu_f = 487 \times 10^{-7} \text{ Pa sec } (327 \times 10^{-7} \text{ lb/ft sec}) \tag{A15}$$

The convection coefficient for a Reynolds number of 2.64×10^5, where $L = 0.0191$ m (0.0625 ft), becomes

$$h_c = 2936 \text{ W/K m } (517 \text{ Btu/hr ft}^2 \text{ °R}) \quad \text{(A16)}$$

By using the temperatures from the previous loop calculations, the material thicknesses, and the material properties of Chung et al. (ref. 6), the following conductivities were calculated:

$t_2 = 1.02$ mm (0.04 in); $t_3 = 1.02$ mm (0.04 in); $t_4 = 0.89$ mm (0.035 in)

$k_2 = 1.65$ W/K m (0.953 Btu/hr ft °R); $k_3 = 10.4$ W/K m (6.0 Btu/hr ft °R);

$$k_4 = 21.1 \text{ W/K m } (12.2 \text{ Btu/hr ft °R}) \quad \text{(A17)}$$

Substituting into equation (A1), we get

$$q'' = 0.69 \text{ MW/m}^2 \ (0.212 \text{ MBtu/hr ft}^2) \quad \text{(A18)}$$

Finally the iterated assumption for T_b was checked by using

$$T_d = T_e + \left(\frac{t_4}{k_4}\right) q'' = 702 \text{ K } (1264 \text{ °R}) \quad \text{(A19)}$$

$$T_c = T_d + \left(\frac{t_3}{k_3}\right) q'' = 768 \text{ K } (1382 \text{ °R}) \quad \text{(A20)}$$

$$T_b = T_c + \left(\frac{t_2}{k_2}\right) q'' = 1180 \text{ K } (2124 \text{ °R}) \quad \text{(A21)}$$

or

$$T_b = T_a + \frac{q''}{h_c} = 1180 \text{ K } (2124 \text{ °R}) \quad \text{(A22)}$$

Since the calculated value of T_b matches the previous loop value, the calculation is converged.

Idle power. The computational procedure for idle power is the same as that for intermediate power. With $h_c = 1190$ W/m^2 K (210 Btu/hr ft^2 °R) the heat flux is 0.296 MW/m^2 (0.094 MBtu/hr ft^2).

Transient Analysis

The transient T-700 engine analysis was based on the following assumptions:

(1) The major transients of interest are ambient (i.e., the condition just prior to engine lightoff) to idle and idle to intermediate power; the cooldown transient computations are the same.

(2) In an engine test, 30 sec would be used in bringing the engine from ambient to idle, and 4 sec would be the shortest time required for a transient from idle to intermediate power. In this analysis an extremely conservative approach will be taken by assuming step changes in temperature and thereby disregarding the more realistic time intervals.

(3) Since the initial flux felt on the surface of the ceramic is required for analysis, the following formula will be sufficient:

$$q''_{trans} = h_c(T_{high} - T_{low}) \tag{A23}$$

where T_{high} is the high value of the step change in $T_{s,4.1}$ and T_{low} is the surface temperature corresponding to the low value of $T_{4.1}$.

Ambient to idle power. If the transient condition is created by a step change of $T_{s,4.1}$ from ambient to idle,

$$T_{high} = 1019 \text{ K } (1835 \text{ °R}); \quad T_{low} = 294 \text{ K } (530 \text{ °R}) \tag{A24}$$

With a decrease in T_f, h_c (Eq. 17)) increases

$$h_c = 1.3 \times 1190 = 1550 \text{ W/m}^2 \text{ K } (273 \text{ Btu/hr ft}^2 \text{ °R}) \tag{A25}$$

and the heat flux becomes

$$q''_{trans} = 1.123 \text{ MW/m}^2 \text{ } (0.356 \text{ MBtu/hr ft}^2) \tag{A26}$$

Idle to intermediate power. Again for a step change in $T_{s,4.1}$

$$T_{high} = 1408 \text{ K } (2534 \text{ °R}); \quad T_{low} = 770 \text{ K } (1387 \text{ °R}) \tag{A27}$$

With a decrease in T_f, h_c (eq. (A17)) increases

$$h_c = 1.1 \times 2936 = 3230 \text{ W/m}^2 \text{ K } (569 \text{ Btu/hr ft}^2 \text{ °R}) \tag{A28}$$

and the heat flux becomes

$$q''_{trans} = 2.06 \text{ MW/m}^2 \text{ } (0.653 \text{ MBtu/hr ft}^2) \tag{A29}$$

APPENDIX B

RIBBON-BURNER ANALYSIS

Steady-State Analysis

The steady-state ribbon-burner analysis is based on the following assumptions:

(1) The conduction equations and the quasi-one-dimensional model of appendix A apply through a semi-infinite slab.
(2) Surface conditions are uniform on the front and back sides with no contact resistance between materials.

The ribbon-burner heat transfer model (fig. 4) is quite similar to the model for the T-700 shroud (fig. 3). The surface temperature (1647 K; 2965 °R) and the embedded thermocouple temperature (947 K; 1705 °R) are measured. The material properties are determined from the curve fits (ref. 6) used in appendix A. The heat flux is calculated by using equation (A1).

$$q'' = \frac{T_s - T_a}{\frac{t_2}{k_2} + \frac{t_3}{k_3} + \frac{t_4}{k_4}}$$

$$= \frac{(1647 - 947)}{0.000562} = 1.25 \text{ MW/m}^2$$

$$= \frac{2965 - 1705}{0.00319} = 0.395 \text{ MBtu/hr ft}^2 \qquad \text{(B1)}$$

$$h_c = \frac{q''}{2280 - 1650} = 1980 \text{ W/m}^2$$

$$= \frac{q''}{4100 - 2965} = 348 \text{ Btu/hr ft}^2 \text{ °R} \qquad \text{(B2)}$$

The convective coefficient can be estimated from q". Given the flame temperature of 2280 K (4100 °R) and the surface temperature of 1647 K (2965 °R)

$$q''_{trans} = 1980 (2280 - 780) = 2.96 \text{ MW/m}^2$$

$$= 348 (4100 - 1400) = 0.940 \text{ MBtu/hr ft}^2 \qquad \text{(B3)}$$

Transient Analysis

The transient ribbon-burner analysis is based on the following assumptions:

(1) The transient case is a virtual step function since the test article is pneumatically forced into the flame stream for each cycle with almost no delay between the cooling station and the hot flame.

(2) Once again, the initial surface flux is the only transient flux of interest.

(3) The convective heat transfer coefficient under the transient conditions will be no smaller than that calculated in the steady-state solutions.

(4) Since the measured ambient surface temperature on the test article was 720 K (1300 °R), the ambient surface temperature will be no greater than 780 K (1400 °R). (The 56 deg K (100 deg R) variance is used as a conservative measure.)

Using the convective heat transfer coefficient (eq. (B2)) and the flame and surface temperatures gives the heat flux as

$$q''_{trans} = 1980\ (2280 - 780) = 2.96\ MW/m^2$$

$$= 348\ (4100 - 1400) = 0.940\ MBtu/hr\ ft^2 \qquad (B3)$$

REFERENCES

1. T.J. Biesiadny, G.A. Klann, E.S. Lassow, M. McHenry, G. McDonald, and R.C. Hendricks, "Experimental and Analytical Study of Ceramic Seals for Turbojet Engines," presented at 9th Annual Conference on Composites and Advanced Ceramics Materials Cocoa Beach, Florida, Jan. 1985.

2. R.C. Bill, D.W. Wisander, and D.E. Brewe, "Preliminary Study of Methods for Providing Thermal Shock Resistance to Plasma Sprayed Ceramic Gas-Path Seals," NASA TP-1561, May 1980.

3. R.P. Incropera, and D.P. DeWitt, "Fundamentals of Heat Transfer." John Wiley and Son, New York, 1981.

4. J.E.A. John, Gas Dynamics. Allyn and Bacon Inc., Boston, 1969.

5. J.H. Keenan, J. Chao, and J. Kay, Gas Tables, 2nd ed. John Wiley and Sons, New York, 1980.

6. B.T.F. Chung, M.M. Kermani, M.J. Braun, J. Padovan, and R.C. Hendricks, "Heat Transfer in Thermal Barrier Coated Rods with Circumferential and Radial Temperature Gradients," ASME Paper 84-GT-181, June 1984.

TABLE I. - IDLE AND INTERMEDIATE STEADY-STATE HEAT TRANSFER CONDITIONS

Parameter	Operating condition	
	Idle	Intermediate[a]
Mach number, M	0.285	0.3
Velocity of flow causing convection, u, m/sec (ft/sec)	182 (598)	226 (740)
Reynolds number	1.8×10^5	2.64×10^5
Temperature of ceramic surface, T_b, K (°R)	771 (1387)	1180 (2124)
Convection coefficient, h_c, W/m^2 K (Btu/hr ft^2 °R)	1192 (210)	2936 (517)
Heat flux, q", MW/m^2 (MBtu/hr ft^2)	0.296 (0.094)	0.669 (0.212)

[a]Intermediate power refers to the maximum power condition for 30 min; the intermediate power temperature used herein is lower than a production model, perhaps high power would be a better description.

TABLE II. - QUASI-STEADY HEAT TRANSFER FOR T-700 ENGINE CONDITIONS

Parameter	Operating condition	
	Ambient to idle	Idle to intermediate
Temperature of gas stream or flame causing transients, T_{high}, K (°R)	1019 (1835)	1408 (2534)
Temperature of ceramic surface just prior to transient effect of T_{high}, K (°R)	294 (530)	771 (1387)
Convection coefficient, h_c, W/m^{2}K (Btu/hr ft^2 °R)	1550 (273)	3231 (569)
Heat flux, q", MW/m^2 (MBtu/hr ft^2)	1.12 (0.356)	2.06 (0.653)

TABLE III. - HEAT FLUX FOR T-700 TEST AND BURNER SIMULATION

Category of heat transfer	T-700 shroud section		Ribbon-burner simulation	
	Heat flux, q"			
	MW/m^2	MBtu/hr ft^2	MW/m^2	MBtu/hr ft^2
Steady state:				
Idle	0.296	0.094	1.25	0.395
Intermediate	.669	.212		
Transient:				
Ambient to idle	1.123	.356	2.97	.940
Idle to intermediate	2.06	.653		

TABLE IV. - STEADY-STATE TEST DATA FOR T-700 ENGINE

Parameter	Idle (run 2223)	Intermediate (run 2224)
Total temperature at station 4.1, $T_{T,4.1}$, K (°R)	1036 (1864)	1433 (2580)
Total temperature at station 3.0, $T_{T,3.0}$, K (°R)	457 (822)	652 (1173)
Total pressure at station 4.0, $P_{T,4.0}$, MPa (psia)	0.36 (52.3)	1.18 (171)
Airflow at station 4.1, $W_{4.1}$, kg/sec (lb/sec)	1.15 (2.53)	3.33 (7.35)

TABLE V. - CALCULATED VELOCITY AT STATION 4.1

Parameter	Idle (run 2223)	Intermediate (run 2224)
Static temperature at station 4.1, $T_{s,4.1}$, K (°R)	1019 (1835)	1408 (2534)
Velocity of flow causing convection, u, m/sec (ft/sec)	332 (598)	411 (740)
Mach number, M	0.285	0.3

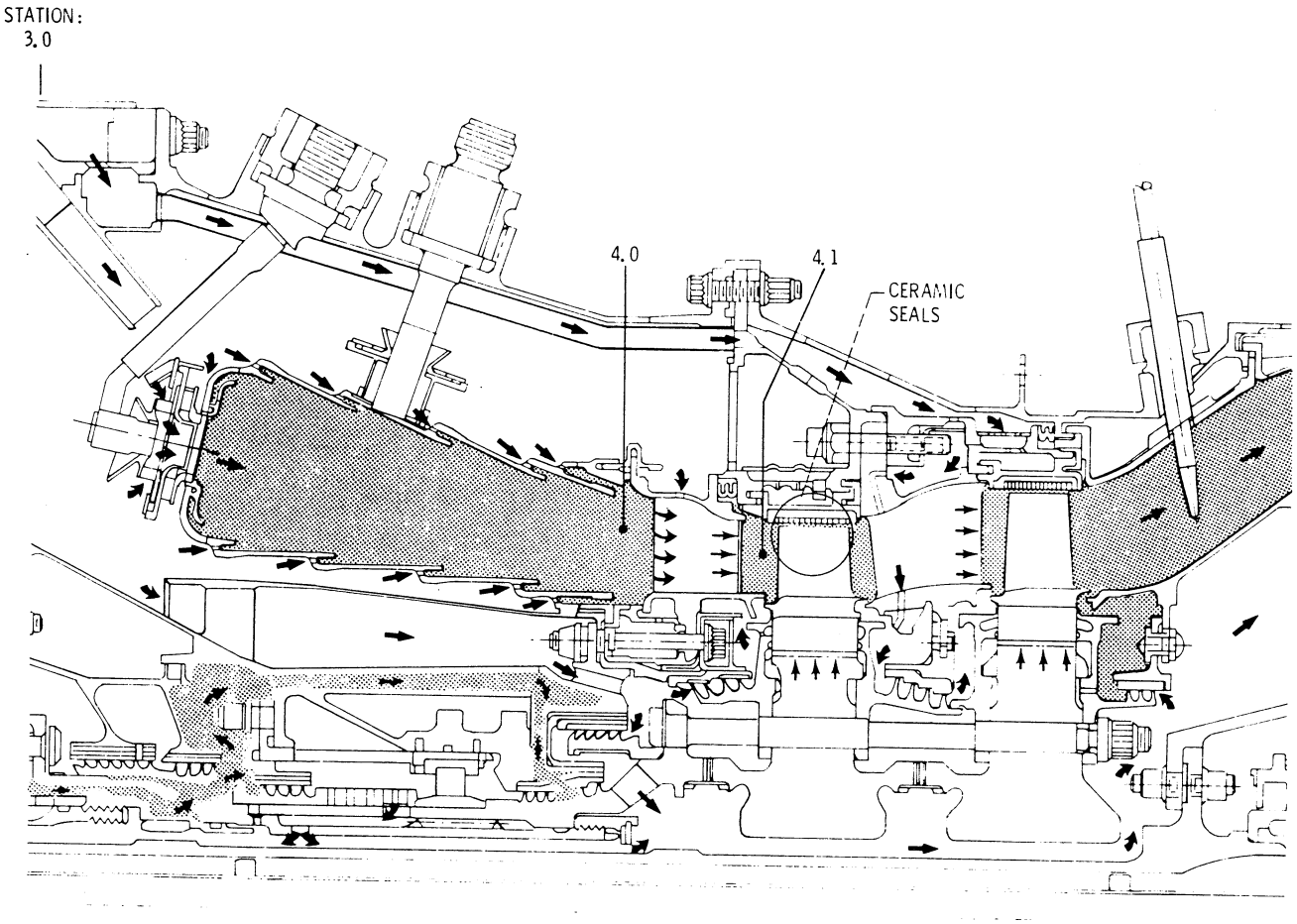

Figure 1. - Schematic of T-700 engine with stations noted.

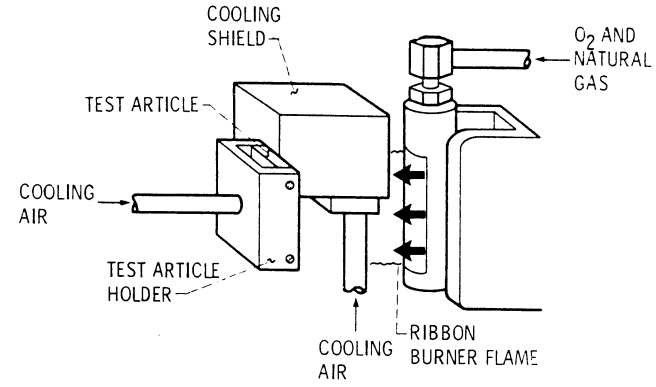

(a) Sketch.

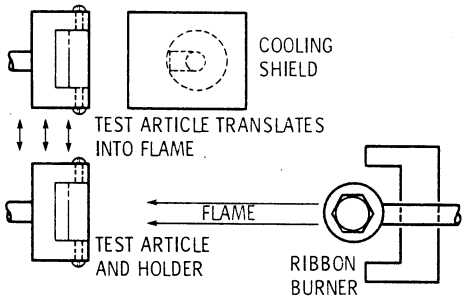

(b) Top view.

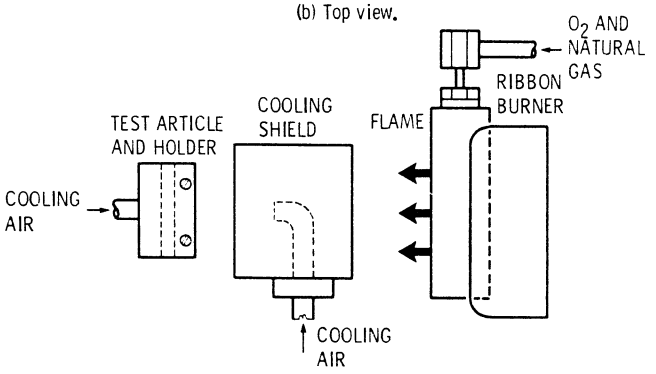

(c) Side view.

Figure 2. - Conceptual representation of ribbon burner.

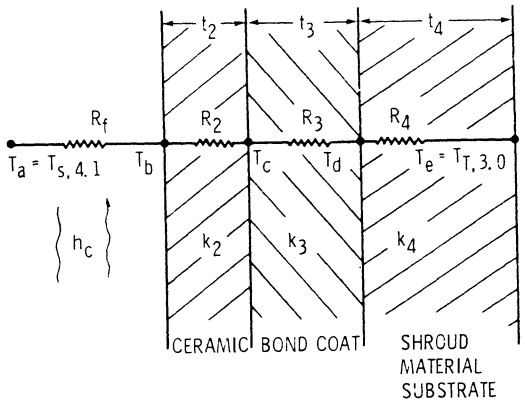

Figure 3. - Heat transfer model for T-700 shroud seal specimen.

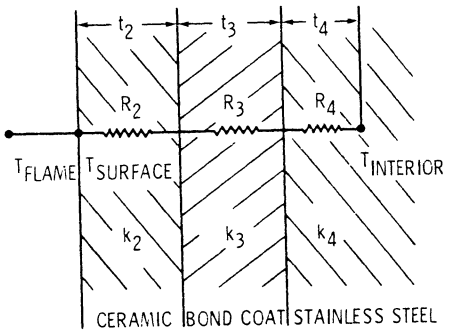

Figure 4. - Heat transfer model for ribbon-burner specimen.

1. Report No.	2. Government Accession No.	3. Recipient's Catalog No.
NASA TM-86940		

4. Title and Subtitle	5. Report Date
Ribbon-Burner Simulation of T-700 Turbine Shroud for Ceramic-Lined Seals Research	6. Performing Organization Code: 505-40-5A

7. Author(s)	8. Performing Organization Report No.
J.K. Little, G.P. Allen, G. McDonald, and R.C. Hendricks	E-2458
	10. Work Unit No.

9. Performing Organization Name and Address	11. Contract or Grant No.
National Aeronautics and Space Administration Lewis Research Center Cleveland, Ohio 44135	13. Type of Report and Period Covered: Technical Memorandum

12. Sponsoring Agency Name and Address	14. Sponsoring Agency Code
National Aeronautics and Space Administration Washington, D.C. 20546	

15. Supplementary Notes

Prepared for the Ninth Annual Conference on Composites and Advanced Ceramic Materials sponsored by the American Ceramic Society, Cocoa Beach, Florida, January 20-24, 1985. J.K. Little, Arnold Air Force Station, Tullahoma, Tennessee 37389; G.P. Allen, G. McDonald, and R.C. Hendricks, NASA Lewis Research Center.

16. Abstract

Experimental and analytical studies were conducted to determine the acceptability of a ribbon-burner simulation of engine conditions for testing ceramic-lined turbine tip shrouds. The calculated values reveal that the ribbon burner establishes at least as harsh a thermal environment as is present at any time within the turbine shroud. Comparisons were made with ceramic components in a turboshaft engine.

17. Key Words (Suggested by Author(s))	18. Distribution Statement
Seal; Coatings; Ceramic; Heat transfer; Testing	Unclassified - unlimited STAR Category 34

19. Security Classif. (of this report)	20. Security Classif. (of this page)	21. No. of pages	22. Price*
Unclassified	Unclassified		

*For sale by the National Technical Information Service, Springfield, Virginia 22161